Study on Ultimate Bearing Capacity of New Spiral Steel Pipe Pile

Hui Zhang[a], Yanpeng Zhu[*], Jiahui Zhu[b], Anping Huang[c], Linping Wu[d], Jinxin Fan[e]

Lanzhou University of Technology

[a]E-mail: 835444817@qq.com, [*]E-mail: zhuyp1@163.com
[b]E-mail: 1056395821@qq.com, [c]E-mail: huanganping1995@163.com
[d]E-mail: wlping0916@163.com, [e]E-mail: Fjx_geometry98@163.com

ABSTRACT. The traditional vane spiral steel pipe pile falls short of meeting the required bearing capacity, necessitating an enhancement in the geometric structure. As such, this paper proposed a novel spiral steel pipe pile with a variable vane diameter is proposed, for which a comprehensive field test was conducted, comprising six groups of compression tests and six groups of uplift tests, each consisting of one compressive pile and two uplift piles. These tests aim to investigate the impact of blade spacing and blade diameter on the bearing capacity. To validate the precision and accuracy of the model, we utilized numerical simulation software for modeling and compared the results with the measured data. In conjunction with the findings from the field test and numerical simulation, the enhancement effect on the ultimate bearing capacity of the improved new steel pipe spiral pile was analyzed. The study reveals that variations in pile type parameters significantly impact the bearing capacity, with the gradual change of blade diameter showing a positive correlation with the ultimate bearing capacity of the spiral steel pipe pile. Additionally, blade spacing plays a crucial role in determining the bearing mode of the spiral steel pipe pile, making changes in blade spacing equally influential on its ultimate bearing capacity. Notably, when considering the equal amount of steel consumption, the new spiral steel pipe pile demonstrates significant improvements in comparison to the traditional counterpart. Specifically, it showcases a substantial increase of approximately 28% in compression bearing capacity and a remarkable uplift bearing capacity boost of about 13%. These investigations substantiated the feasibility of using ABAQUS numerical simulation software to analyze the bearing capacity of the new spiral steel pipe pile and the reliability of its application in foundations with uneven bearing capacity in rural housing construction. As a consequence, these findings provide a valuable theoretical basis for implementing the new spiral steel pipe pile in rural housing construction projects.

Keywords: New spiral steel pipe pile; Ultimate bearing capacity; Field test; Numerical simulation analysis; Pile type parameter

Z. Ahmad et al. (eds.), *Proceedings of the 2023 5th International Conference on Structural Seismic and Civil Engineering Research (ICSSCER 2023)*, Atlantis Highlights in Engineering 24,
https://doi.org/10.2991/978-94-6463-312-2_23

1 Introduction

The vane spiral steel pipe pile enhances its compression and uplift bearing capacity through the incorporation of blades into the pile body. This innovative design offers several functional advantages, including swift construction, the flexibility of multi-angle installation (horizontal, vertical, or any desired angle), recyclability, environmental friendliness, and cost-effectiveness [1-2]. As a result, the vane spiral steel pipe pile holds tremendous potential for widespread development and application in various construction projects.

Differing from the traditional spiral steel pipe pile with an equal blade diameter, the new spiral steel pipe pile with blade type exhibits a higher level of complexity. The ultimate bearing capacity of the pile is notably subject to changes in its geometric parameters, leading to intricate characteristics and mechanisms. In contrast, the traditional spiral steel pipe pile with equal blade diameter has a more straightforward behavior. Vane spiral steel pipe pile is an engineering invention in the middle and late 19th century. In 1833, Michelle [3] filed a patent application in London for what was initially known as the spiral steel pipe pile. Later, in 1961, Balla [4] presented the shape of the soil slip surface for the spiral pile blade, approximating it to be round. During this study, it was observed that the uplift capacity of this model was influenced by both the weight of the pile and the soil, as well as the friction between the soil and the curved surface. The theoretical formula used was based on soil slip theory, but it became apparent that the accuracy of the soil slip model for spiral anchors necessitated improvement. In 1967, Adams [5] experimentally investigated the relationship between the torque of a spiral pile in the rotating stage and the uplift force of a spiral pile and derived a bearing capacity formula for the pile in terms of the uplift force. However, this formula is subject to significant variations due to soil material properties, pile rotation conditions, and pile size, and as such, it fails to provide precise solutions. To address this limitation, extensive axial field load tests have been conducted on individual spiral steel pipe piles with an axial diameter (d) exceeding 150 mm [6-10].

The bearing capacity of spiral steel pipe piles depends on pile type parameters and foundation strength to a great extent. Chance Company [11] studied the influence of different pile type parameters on the bearing capacity of piles through a large number of field tests. Their findings revealed that for layered blade piles, an optimum blade spacing occurs when it is approximately three times the blade diameter of the spiral steel pipe pile. This conFigureuration results in the highest bearing capacity of the piles. Another crucial pile type parameter that plays a key role in determining the final foundation failure mode of vane steel pipe spiral steel pipe piles is the blade spacing to diameter ratio (S/D). Taking inspiration from the simple analysis model of Rao et al. [12], Stanier et al. [13] used transparent soil and laser-assisted PIV in 2013 to study the failure mechanism of spiral steel pipe pile with S/D in the range of 1.5-3.0. In 2017, Malik [14] et al. made a comparative analysis of the end-bearing capacity of spiral steel pipe piles and straight piles under similar geological conditions through a sandbox test, and they found that under similar pile tip area and grounding conditions, the ultimate bearing capacity of the small spiral pile with single spiral is 16.25% lower than that of

straight pipe pile on average. According to the test results, the traditional formula for calculating the bearing capacity of spiral steel pipe pile tip was modified and reduced. The research on the ultimate bearing capacity of spiral steel pipe piles has attracted a lot of attention from scholars in China. Most of the research methods are theoretical calculation, numerical analysis, model tests, and practical engineering observation. Liu [15], Li [16], and Dong et al. [17-18] have conducted comprehensive and systematic research on spiral steel pipe piles, both theoretically and experimentally. Their work has resulted in the development of calculation methods for determining the bearing capacity of spiral steel pipe piles under both compression and uplift conditions. To explore the influence of various factors on the bearing capacity, these researchers conducted experiments where they altered certain geometric parameters of the piles. However, the insufficient number of tested piles leads to some incompleteness in the range of geometric parameters considered in the experiments.

At present, the traditional vane spiral steel pipe pile is generally designed with equal blade size and equal spacing. In view of the uneven bearing capacity of the foundation arising from the influence of miscellaneous fill in the surface layer of the foundation in the construction of villages and towns, this paper designed six new types of vane spiral steel pipe piles, and studied the influence of pile type parameters such as blade spacing and blade diameter on the ultimate bearing capacity of the new type of vane spiral steel pipe piles through static load tests. This study can provide data support and a theoretical basis for the new spiral steel pipe pile in the construction of rural buildings with uneven foundation-bearing capacity.

2 Field test of new spiral steel pipe pile

2.1 Test site overview

The test site is situated in Pengjiaping Town, Qilihe District, Lanzhou City, Gansu Province. It falls within the advanced terrace category on the southern bank of the Yellow River. Upon conducting the survey, it was observed that the topography of the site slopes higher towards the south and gradually descends towards the north, with a ground elevation ranging from 1596.34 to 1597.89 meters. Originally used for cultivation, the site's upper soil layer mainly consists of cultivated soil or miscellaneous fill. In contrast, the undisturbed soil layer comprises aeolian loess, resulting in a foundation with poor bearing capacity and porous, loose soil characteristics. Consequently, prior to conducting the test, a 1-meter excavation was carried out to remove the surface miscellaneous fill. The thickness of the miscellaneous fill layer was measured to be 1.2 meters. The excavation area covered a space of 10.0 meters by 10.0 meters, with a 1.5-meter distance between each test pile. The remaining area served as the designated working space for the excavator. Figure. 1 depicts a visual representation of the site excavation and pile test layout. The soil layers at the site are organized in a specific sequence, starting from the top and going downwards. The uppermost layer is a filling layer consisting mainly of silty clay, with a thickness of approximately 2.2 meters. Below that, there is a layer of loess-like silt, featuring white calcareous stripes and measuring about 2.2 meters in thickness. Following this, there is a silty clay layer with

ferruginous stripes, which is approximately 2.6 meters thick. Lastly, there is a layer of silty fine sand that contains quartz, feldspar, mica, and silty clay, with a thickness of around 1.9 meters. During the field bearing capacity test of vane spiral steel pipe piles, a pile-type comparison test was conducted, dividing the test into six sub-groups, each comprising three piles. This resulted in a total of 18 test piles, with a pitch (P) of 102 millimeters between each test pile. The spiral steel pipe pile used in the test is shown in Figure. 2.

Fig. 1. On-site excavation and test pile layout.

Fig. 2. Finished test pile.

2.2 Soil parameters

Samples were excavated from the project site, and indoor geotechnical tests were carried out according to the Standard for Geotechnical Test Methods (GB/T50123-2019) to determine the physical and mechanical parameters of the soil layer (Table 1).

Table 1. Physical and mechanical parameters of on-site soil layers.

Name	Compression modulus /MPa	Poisson's ratio	Cohesion /kPa	Internal friction Angle /(°)	Soil layer thickness /m
Miscellaneous fill	4	0.2	10.32	15.3	1.2
Loess-like silt	10	0.4	15	25.24	2.0

2.3 Pile type parameters

These test piles share the same specifications with a length (L) of 1.6 m and a diameter (d) of 60 mm. However, there are three different blade diameters (D) available: 200 mm, 150 mm, and 250 mm. The pitch (P) between the test piles is maintained at 102 mm. The material used for these piles is Q235B, and both the inside and outside surfaces are hot-dip galvanized to prevent corrosion effectively. The parameters representing different pile types are illustrated in Figure. 3, and Table 2 provides a detailed breakdown of the specific pile type parameters. In total, 18 test piles were used in this study, with each group consisting of three custom piles.

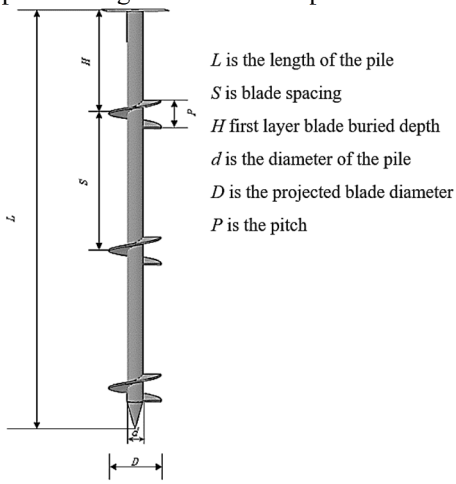

Fig. 3. Parameters of a new spiral steel pipe pile.

Fig. 4. Professional piling. equipment.

Table 2. Table of pile type parameters.

Pile No.	Pile length *L*/m	Pile diameter *d*/mm	Blade diameter *D*/mm			Number of blades	Blade spacing *S*/mm			Number of test piles
			First lane (mm)	Second lane (mm)	Third lane (mm)		First lane (mm)	Second lane (mm)	Third lane (mm)	
a1	1.6	60	200	200	200	3	100	625	1150	3
b1	1.6	60	200	200	200	3	100	550	1150	3
a2	1.6	60	150	200	250	3	100	625	1150	3
b2	1.6	60	150	200	250	3	100	550	1150	3
a3	1.6	60	250	200	150	3	100	625	1150	3
b3	1.6	60	250	200	150	3	100	700	1150	3

2.4 Field Test

In adherence to the layout and distribution shown in Figure. 1, the prefabricated vane spiral pipe steel pipe piles were screwed into the ground using specialized piling equipment via applying torque. The process involves the use of professional piling equipment, as illustrated in Figure. 4.

The test loading method adopts the anchor pile method, and the test device is shown in Figure. 5. During the loading process, a 160 kN hydraulic jack (showing tonnage pressure value) was used to press, the middle test pile bore downward compression bearing capacity, and the test piles at both ends bore upward uplift force through steel wire rope. The upward uplift force was directly read out by a tension meter, and the vertical deformation of the test pile during loading was measured by a displacement meter with a measuring range of 50.0 mm. Two displacement meters were symmetrically arranged at the top of the test pile, and the average displacement was taken.

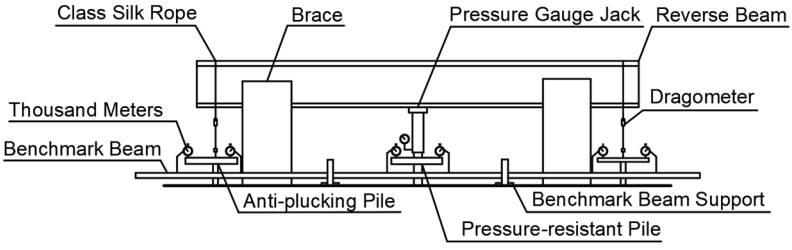

Fig. 5. Schematic diagram of uplift and compression test device.

In the test, the slow sustaining load method was used to load, and the design load was determined according to the estimated ultimate bearing capacity of a single pile, and the single stage load of the test was 1/10 ~ 1/8 of the design load. (1) When the displacement of the pile top is greater than 5.0 times the displacement of the previous load after applying this load; (2) When the cumulative displacement of the pile top is more than 30 mm; (3) When there is an obvious inflection point in the load-displacement

curve (*Q*-*s* curve), the loading can be terminated [19]. In this paper, two indexes (2) and (3) were used to judge the ultimate bearing capacity of pile foundations.
After the test, the test pile was dismantled and recovered, and the process of pile dismantling was observed.

2.5 Analysis of test results

(1) Analysis of compression test results.

By sorting out the compression bearing capacity data of six pile types, we have plotted the *Q*-*s* curves for the single pile static load test, as depicted in Figure. 6, from which it is apparent that the curves of the six pile types exhibit a similar trend. However, a noticeable difference is observed in the settlement between pile a3 and pile a2 under identical load conditions. Specifically, pile a3 demonstrates a lower settlement compared to pile a2 for the same applied load. At the calibration displacement of 30 mm, the bearing capacity of pile a3 is 12.5% higher than that of pile a2 and 28.6% higher than that of pile a1. During the initial loading stages, the curves of piles b2 and b3 display a similar trend. However, as the cumulative displacement reaches 30 mm, pile b3 surpasses pile b2 in terms of bearing capacity. Whereas the second inflection point of smoothing all pile curves is not obvious, all pile curves have undergone a processing step. Here, the lg*Q*-*s* curve is selected for drawing, as shown in Figure. 7.

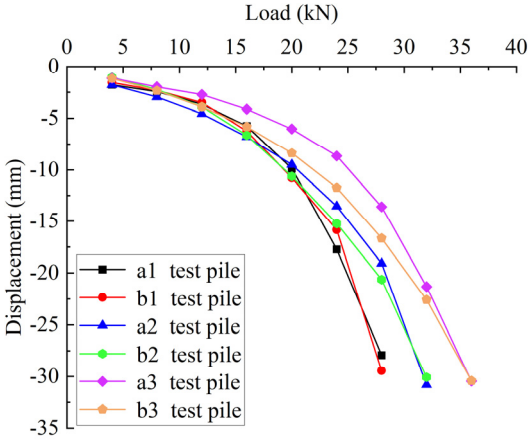

Fig. 6. Q-s curves of compression resistance of test piles.

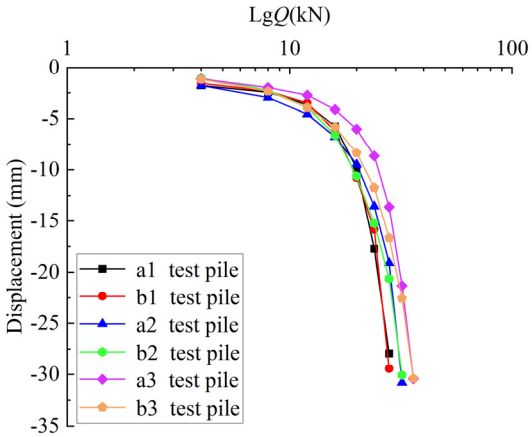

Fig. 7. lgQ-s curves of compression resistance of test piles.

(2) Statistics and processing of uplift test data.

By sorting out the data of uplift bearing capacity of six pile types, the *Q-s* curve is plotted as shown in Figure. 8. From Figure. 8, we can observe that the displacement and settlement trends of piles a1, b1, a2, a3, b2, and b3 show similar behavior when the load is low. However, as the load increases, pile b1 experiences a significant decrease in its uplift bearing capacity, and a second inflection point becomes evident. On the other hand, the curves for the remaining piles still exhibit gentle and smooth trends, without a clear second inflection point. The lg*Q-s* curve is selected for drawing here, as outlined in Figure. 9.

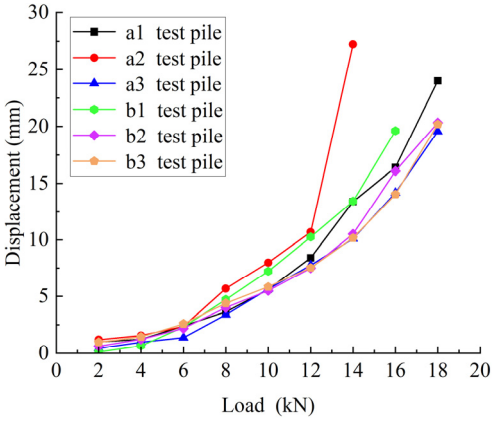

Fig. 8. Q-s curves of uplift resistance of test piles.

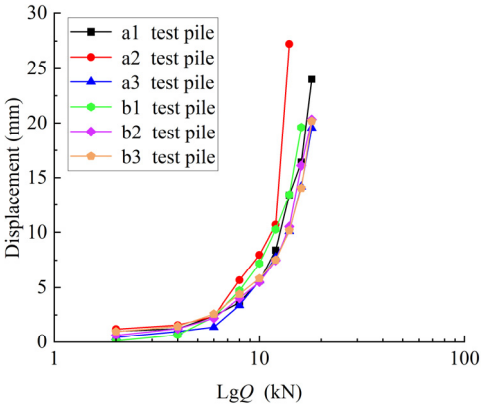

Fig. 9. lgQ-s curves of uplift resistance of test piles.

The comparison between piles a1 and b1 reveals that when the blade spacing of spiral steel pipe piles is not equal, the influence on the ultimate compression bearing capacity is minimal, but the influence on the uplift ultimate bearing capacity is prominent. The design of equal pitch in a spiral steel pipe pile ensures that the screw-in track of the lower blade aligns with that of the upper blade, resulting in minimal disturbance to the surrounding soil during installation. Consequently, for piles with the same blade diameter, a spiral steel pipe pile with equal blade spacing tends to have a higher bearing capacity compared to a spiral steel pipe pile with variable blade spacing. When comparing the uplift bearing capacity of piles a3 and b3, their similar performance can be attributed to the specific design of their blades, where the first blade has the largest diameter, and as the blades are positioned closer to the surface, their diameters progressively decrease. This design characteristic results in reduced disturbance to the soil caused by the first blade compared to the blades above it, leading to a diminishing effect of the variable blade spacing on soil disturbance. Thus, the difference in bearing capacity between spiral steel pipe piles with variable blade spacing and those with equal blade spacing becomes less pronounced.

(3) Analysis and observation of pile dismantling.

After conducting the bearing capacity test, we proceeded to meticulously pull out and dismantle the spiral steel pipe pile. In the process of disassembly and assembly, we recorded and analyzed the pulling process and the results after pulling out of the spiral steel pipe pile.

It is notable from Figure. 10 that there is a complete soil cylinder between the blades of the spiral steel pipe pile after pulling out, and the soil is a shear failure during pulling out, which is the cylindrical shear mode at this time. However, there is no complete cylindrical soil column on the uppermost blade, which also proves that the uppermost blade is a blade-bearing mode. It is evident from Figure. 11 that the soil between blades is compacted, which also proves that spiral steel pipe piles can exert their soil-squeezing effect in slope and road reinforcement, and it is a foundation form with a wide application range.

Fig. 10. Piles removal.

a) Main view of soil column between blades.

b) Left view of soil column between blades.

Fig. 11. Soil column between blades.

3 Numerical simulation of new spiral steel pipe pile

Based on the general numerical simulation analysis software ABAQUS, the calculation model of pile-soil interaction was established. In this simulation study, a new three-dimensional model of a spiral steel pipe pile with the same size as the field test was adopted, and the three-dimensional model of soil was established according to the basic data of soil obtained from the actual site geological prospecting report and laboratory test. The general modeling principle is that the influence of soil boundary on the simulation results is considered in the simulation, the soil depth is twice the pile length, and the soil radius is 10 times the maximum blade radius.

The following is a brief description of the model establishment and calculation process.

(1) The partition of model units.

The grid division of the whole model is the premise of ensuring the calculation accuracy. To improve the calculation accuracy, the model was divided into regions according to its shape to realize the structural grid division of pile and soil. When setting the grid, the central area was encrypted, and the grid of soil parts cut by blades was encrypted emphatically. Except for the pile tip and pile tip soil, the grid element type of other components was the C3D8R element, and the pile tip and soil around the pile tip were divided by the C3D4 element. Because of different pile types, the number of grids used is also different. To strike a balance between calculation accuracy and computational speed, it is common practice to limit the number of units to approximately 40,000 when conducting simulations of spiral steel pipe piles. Figure. 12 illustrates the grid division diagrams.

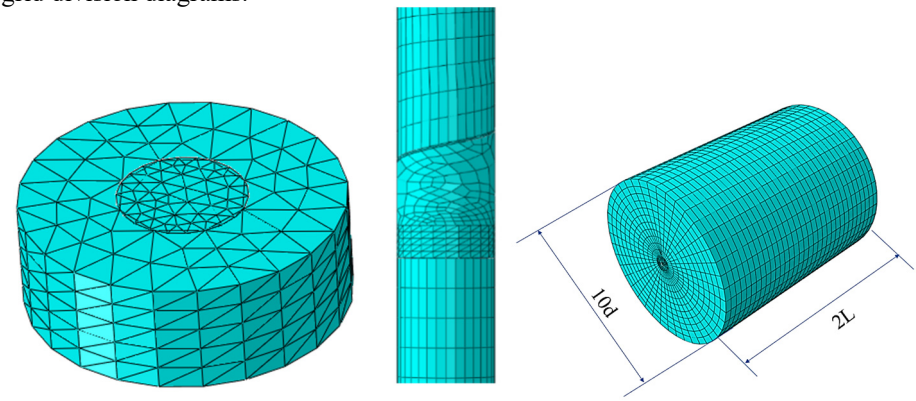

a) Pile tip and pile tip soil grid. b) Cut soil grid. c) Pile tip and pile tip soil grid.

Fig. 12. Numerical simulation grid generation of a new type of spiral steel pipe pile

(2) Material properties.

This study adopts Mohr-Coulomb elastoplastic model as the constitutive model of soil considering the plasticity of soil by selecting the parameters according to the data measured by geotechnical tests. Q235B is endowed with material properties by pile model, with an elastic modulus of 210 MPa and a Poisson's ratio of 0.3. The interface strength was reduced according to the previous research, with a reduction factor of 0.5.

(3) Load and model boundary conditions.

To balance the in-situ stress, a force of -20kN was first applied to the ground stress calculation model. The lateral constraint was applied to restrain the horizontal displacement of soil, but vertical displacement can occur, so the boundary condition adopts normal constraint except the top surface is taken as a free boundary.

(4) Reliability analysis of numerical simulation.

To test the influence of grid division on the test results, numerical analysis tests of single pile compression under different grid division conditions were carried out, and *Q-s* curves obtained from numerical analysis and physical model tests under the same conditions were compared. Figure. 13 displays the comparison between numerical results and simulation results under the optimal grid division conditions, and the two curves are the most consistent. This observation indicates that the test results have a high degree of coincidence within the allowable error range, and the established numerical analysis model can accurately reflect the actual bearing capacity. Therefore, the grid division standard was adopted in the follow-up research.

3.1 Influence of blade diameter change on bearing capacity of spiral steel pipe pile

Figure. 14 and Figure. 15 show the compression and uplift failure modes of the three piles a1, a2 and a3 respectively at the maximum displacement obtained by the numerical model. It is noteworthy that the soil between the spiral blades of the new spiral steel pipe pile has a larger displacement driven by the spiral blades, while the vertical displacement of the soil outside the spiral blades is significantly less than that between the spiral blades, and the shear resistance caused by the relative displacement of the soil between the spiral blades and the soil outside the spiral blades provides the lateral bearing capacity of the spiral steel pipe pile. At the same time, the vertical displacements of the soil between the spiral blades and the pile body are roughly similar, that is, the spiral blades drive the soil between the blades and the pile body to move together, which shows that the new spiral steel pipe pile with three blades can better transfer the load on the top of the pile to the soil around the pile, thus giving full play to the bearing capacity of the soil around the pile.

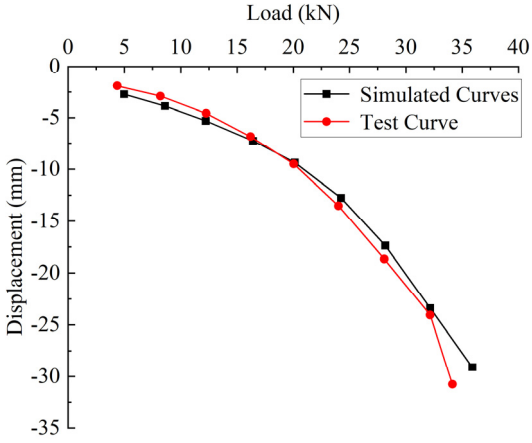

Fig. 13. Comparison of numerical simulation and field test data under optimal grid condition.

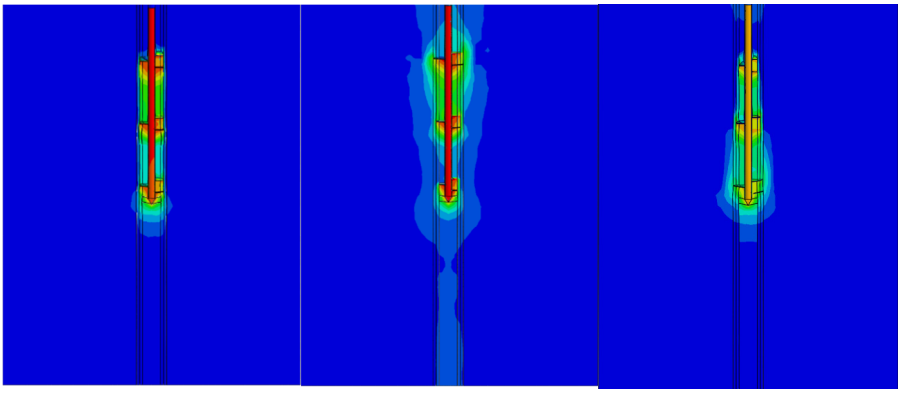

a) pile a1 b) pile a2 c) pile a3

Fig. 14. Vertical compression failure form of pile type a.

It can be observed from Figure. 14 that the failure mode of compressive pile a1 is relatively uniform, which accords with the cylindrical shear failure mode and also aligns with the failure mode obtained from the field test in Figure. 11. However, for the failure modes of compressive piles a2 and a3, especially the soil displacement between the first blade and the second blade shown by pile a2 is very small, which is more in line with the pear-shaped failure mode given by Dong [20] et al. the blade diameter of pile a3 decreases from bottom to top, the damage degree of the first blade to soil is greater than that of the third blade, and the overall damage form is frustum type. With the gradual change of blade diameter, the diffusion range of the slip crack zone also changes. From Figure. 15, it can be noted that the soil deformation zone of uplift pile a1 is relatively regular, the soil displacement zone around uplift pile a3 exhibits a gourd-shaped failure mode, and the soil displacement zone around uplift pile a3 presents a gourd-shaped failure mode.

Figures. 16 and 17 depict the variation of compression and uplift bearing capacity of a single pile with the diameter of spiral blades of piles a1, a2, and a3. The results of the field test and numerical simulation suggest that the change in blade diameter has an obvious influence on the bearing capacity of spiral steel pipe piles. Especially, when the blade diameter increases from top to bottom, the bearing capacity of the spiral steel pipe pile increases significantly. Compared with pile a1, the ultimate compression bearing capacities of piles a2 and a3 increased by 12% and 28% respectively, and the ultimate uplift bearing capacities increased by 16% and 9% respectively. This is because the upper and lower soil layers of the test site were unevenly distributed, and the bearing capacity of the lower loess silt was better than that of the upper miscellaneous fill layer, so the influence of the lower blade diameter on the bearing capacity was more obvious.

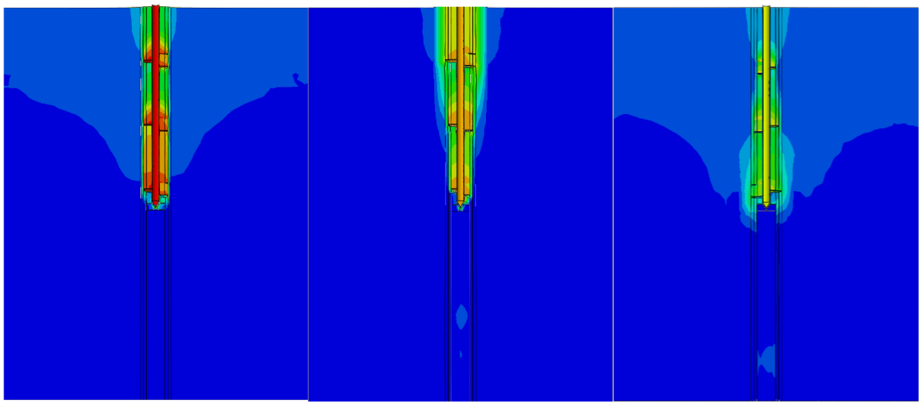

a) pile a1 b) pile a2 c) pile a3

Fig. 15. Vertical uplift failure form of pile type a.

The *Q-s* curves of pile a1 and pile a2 are essentially the same, but for pile a3, there is a big gap between the simulation results and the field test results. The reason is that the soil disturbance is not considered in the simulation test. In the field test, pile a3 has the largest lower blade and the largest disturbance to the soil, which results in the incomplete exertion of the upper blade bearing capacity. As a consequence, this can lead to a large discrepancy between the test results and the simulation results. The comparison between Figures. 16 and 17 demonstrate that it has a greater impact on its uplift bearing capacity.

In practical engineering applications, given the uneven distribution of mixed fill in the upper layer and loess silt in the lower layer of the foundation of villages and towns, the design idea of increasing the blade diameter from top to bottom should be adopted in the design of spiral steel pipe pile to provide higher bearing capacity.

3.2 Influence of blade diameter and spacing on bearing capacity of steel pipe pile

Taking into account the comparison with pile type a, this field test and numerical simulation use three-blade spiral steel pipe pile type b for comparative analysis, and study the influence of blade diameter (D) and blade spacing (S) on the bearing capacity of spiral steel pipe piles. Figures. 18 and 19 are the compression and uplift failure forms of pile type b at the maximum displacement, respectively.

It is observable from Figures. 18 and 19 that with the gradual change of blade spacing, the soil interaction area between blades is closer, and the failure mode of pile b2 is particularly obvious compared with pile a2 in Figure. 15. The compression failure pattern diagram in Figure. 18 indicates that with the gradual change of blade spacing, the diffusion range of slip crack zone also changes gradually. From Figure. 19, it can be found that the expansion of the spacing between the first blade and the second blade enlarges the influence range of the first blade. Therefore, the failure form of pile b3 is larger than that of pile a2, which is consistent with the research results of domestic

researchers on blade spacing. Likewise, a comparison between Figure. 19 and Figure. 11 demonstrates that the simulation results of soil deformation and failure between uplift pile blades are similar to the field test results, and the displacement and deformation range of surface soil increases with the increase of the diameter of the third blade.

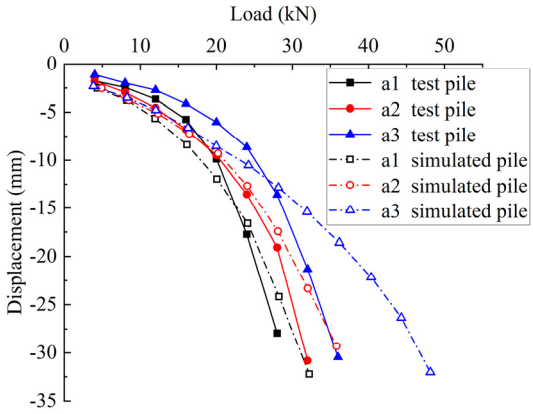

Fig. 16. Q-S curves of compression bearing capacity of pile type a.

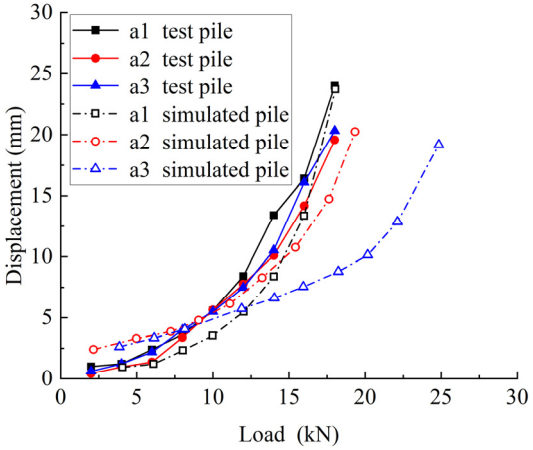

Fig. 17. Q-S curves of uplift capacity of pile type a.

It is observable from Figures. 18 and 19 that with the gradual change of blade spacing, the soil interaction area between blades is closer, and the failure mode of pile b2 is particularly obvious compared with pile a2 in Figure. 15. The compression failure pattern diagram in Figure. 18 indicates that with the gradual change of blade spacing, the diffusion range of slip crack zone also changes gradually. From Figure. 19, it can be found that the expansion of the spacing between the first blade and the second blade enlarges the influence range of the first blade. Therefore, the failure form of pile b3 is larger than that of pile a2, which is consistent with the research results of domestic researchers on blade spacing. Likewise, a comparison between Figure. 19 and Figure.

11 demonstrates that the simulation results of soil deformation and failure between uplift pile blades are similar to the field test results, and the displacement and deformation range of surface soil increases with the increase of the diameter of the third blade.

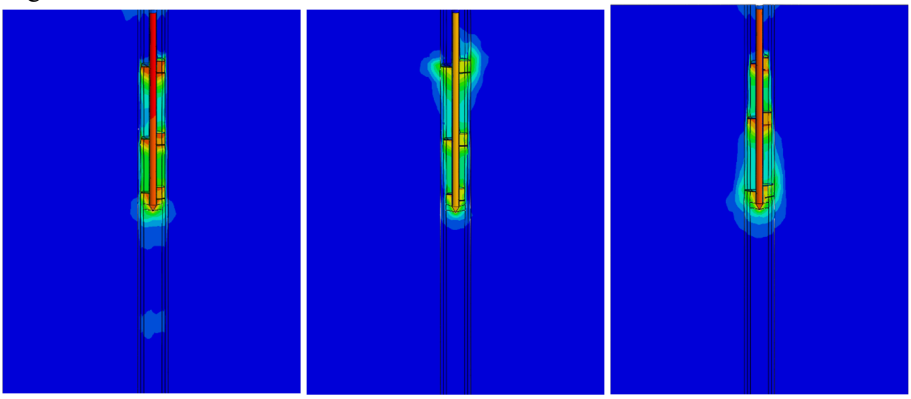

a) pile b1 b) pile b2 c) pile b3

Fig. 18. Vertical compression failure form of pile type b.

The comparison between field test results and numerical simulation results of compression and uplift resistance of pile type b is shown in Figures. 20 and 21 respectively. The comparison results show that the numerical simulation results are roughly consistent with the field test results under the conditions of variable blade spacing and equal blade spacing. The prediction accuracy of the ultimate bearing capacity of piles b1 and b2 is higher than that of the field test results, with an error of less than 5%, but the test result for prediction accuracy of pile b3 is poor, with an error of 17%.

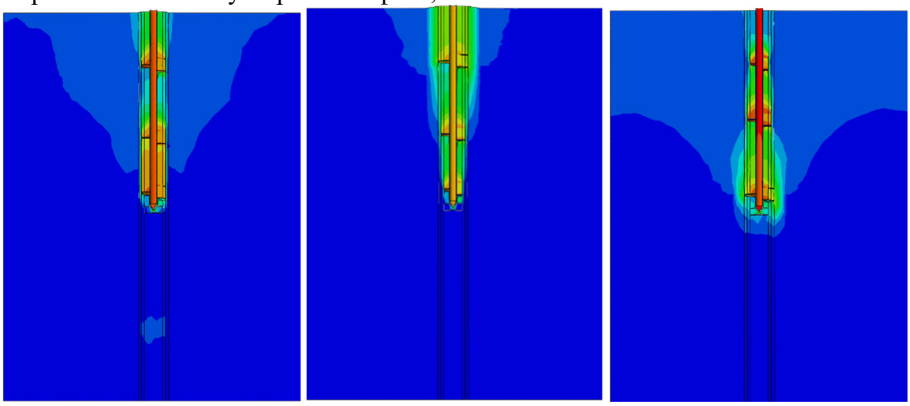

a) pile b1 b) pile b2 c) pile b3

Fig. 19. Vertical uplift failure form of pile type b.

The reason is similar to the error between the results of the field test and numerical simulation of pile a3 in the first group of tests, because the soil disturbance leads to the decrease of the bearing capacity of the field test, while the numerical simulation cannot simulate the influence of soil disturbance on the test results.

It can be seen from Figures. 20 and 21 that the gradual change of blade spacing and the increasing and decreasing of blade diameter will affect the uplift bearing capacity of steel pipe spiral steel pipe pile. However, from the *Q-s* curve of test pile a3 and simulation pile a3 in Figure. 21, it is apparent that when the blade diameter increases from top to bottom, the disturbance to the original soil is greater. Therefore, when this type of pile is used in practical engineering, the simulation results should be used after considering the safety factor to ensure the safety of the superstructure.

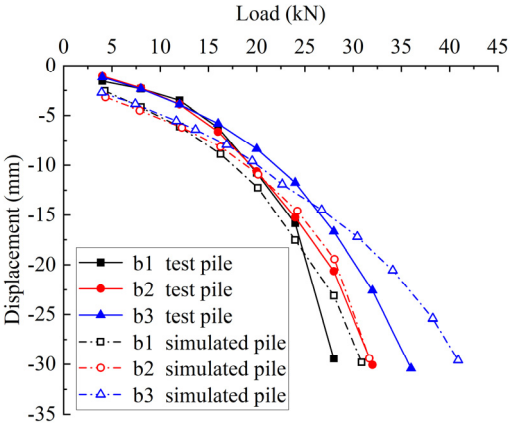

Fig. 20. Q-S curves of compression bearing capacity of pile type b.

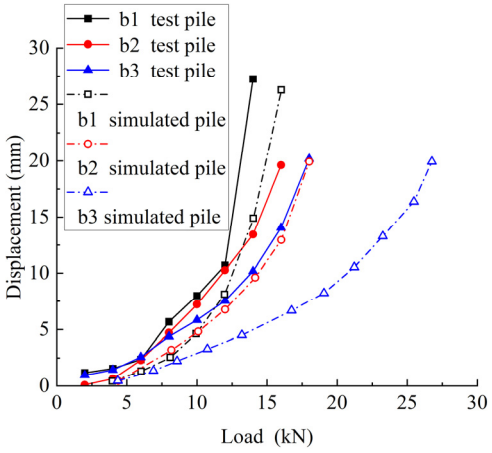

Fig. 21. Q-s curves of uplift capacity of pile type b.

4 Ultimate bearing capacity analysis of new spiral steel pipe pile

The inflection point method and cumulative displacement method are used to determine the ultimate bearing capacity of the spiral steel pipe pile. The comparison of

compression and uplift ultimate bearing capacity obtained from field test and numerical simulation is shown in Table 3 and Figures. 22 and 23, where the data in brackets in Table 3 is the difference percentage between numerical simulation results and field test results.

It is noteworthy from Table 3 and Figure. 22 that the numerical simulation results of the ultimate compression bearing capacity of piles a1, b1, a2 and b2 are all greater than the field test results, and the difference is less than 10%. The analysis of piles a3 and b3 demonstrates that there is a big difference between the numerical simulation results and the field test results. As previously analyzed, the reason is that the disturbance influence of the first blade on the original foundation soil layer is not considered in the simulation process, so the difference between the numerical simulation results and the field test results is larger. As for the ultimate uplift bearing capacity, it is observable from Table 3 and Figure. 23 that there is a big difference between the numerical simulation results of piles b1, a2 and b3 and the test values measured in field tests. By comparison, we found that the predicted results of numerical simulation exceed the field test results by up to 20%. The uplift bearing capacity estimation of piles a1, b2, and a3 is too low, the difference is within 15%. Simply put, the numerical simulation results are consistent with the field test results, and the maximum difference is less than 25%, which shows that the numerical simulation has high prediction accuracy. Therefore, the numerical simulation method can be used to predict the ultimate bearing capacity of the new spiral steel pipe pile in advance in the foundation design of villages and towns.

Table 3. Comparison table of ultimate bearing capacity of spiral steel pipe piles.

Pile type	Field test		Simulation test	
	Compression resistance (kN)	Uplift resistance (kN)	Compression resistance (kN)	Uplift resistance (kN)
a1	25	16.8	26.3 (5.07%)	16.5 (-1.80%)
b1	24.6	14.8	25.8 (4.76%)	18.5 (22.22%)
a2	28	19	29.2 (4.20%)	23.3 (20.33%)
b2	28	16.5	28.3 (1.07%)	14.5 (-12.9%)
a3	32	18.3	37.5 (15.83%)	17.3 (-5.62%)
b3	30.5	19	36.1 (16.82%)	24.3 (24.48%)

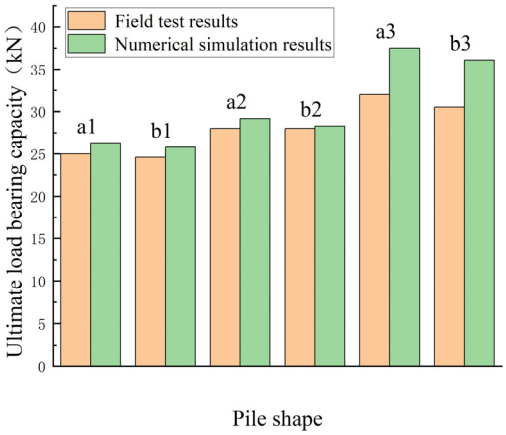

Fig. 22. Comparison of ultimate compression bearing capacity.

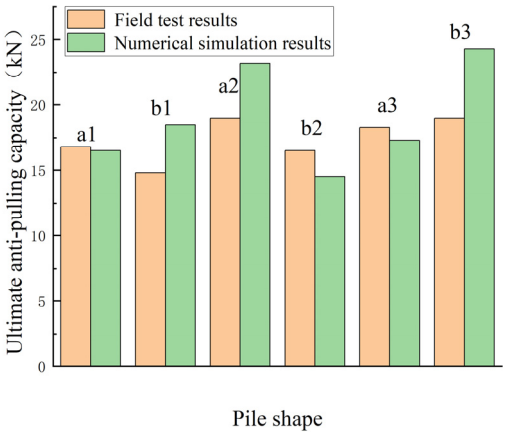

Fig. 23. Comparison of ultimate uplift bearing capacity.

5 Conclusions

In conjunction with the field test and numerical simulation, the study focuses on the influence of geometric parameters on two key aspects: the load-displacement curve and the soil failure mode around the pile. By analyzing these factors, the research reveals valuable insights into the bearing capacity and design considerations for new spiral steel pipe piles in uneven foundations of village buildings. The main conclusions are as follows:

(1) Through the analysis of the test results, we found that the blade spacing of spiral steel pipe piles has a relatively minor impact on compression bearing capacity but significantly affects uplift bearing capacity. Among the piles, a3 demonstrates the best suitability for uneven foundation soil layers in rural buildings. In comparison to a1, pile a3 exhibits a 21% increase in compression bearing capacity, an 8% increase in uplift

bearing capacity, and only a 2% rise in steel consumption. These improvements in bearing capacity are substantial, with minimal cost changes and the added benefit of faster installation, ultimately enhancing construction efficiency.

(2) The successful removal of the test pile provided valuable evidence supporting the reliability of the new spiral steel pipe pile in practical engineering applications. The observation of shearing failure in the soil column between the blades after the pile was pulled out, along with the squeezed and compacted soil between the blades, further substantiates the performance and effectiveness of the new design.

(3) Upon comparing the results of the field test and numerical simulation, a positive correlation has been observed between the blade diameter and the bearing capacity of spiral steel pipe piles. However, it is essential to note that the enlargement of blades can lead to increased disturbance of the original foundation soil, resulting in a decrease in the overall bearing capacity of the foundation. This effect is particularly noticeable in the case of new piles that have a large lower blade diameter and a small upper blade diameter.

(4) The numerical simulation results of each pile type have shown a high level of agreement with the field test results, with the maximum difference being less than 25%. This observation indicates that the numerical simulation method possesses high prediction accuracy and reliability. The numerical simulation method can be confidently employed to predict the ultimate bearing capacity of new spiral steel pipe piles during the foundation design of villages and towns.

Acknowledgement

Fund Project: General Project of National Natural Science Foundation of China (51978321); Changjiang Scholars and Innovation Team Support Program of Ministry of Education (IRT_17R51)

References

1. ADAMS J I, KLYM T W. (1972) A study of anchorages for transmission tower foundations. J. Canadian Geotechnical Journal, 9(1): 89-104.
2. CHANCE CO A B. (2000) Helical pier foundation systems. R Centralia USA: Hubbell Inc.
3. Das B M. (2017) Shallow foundations: Bearing capacity and settlement. 3rd ed. Boca Raton: Taylor & Francis Group.
4. Debnath A, Singh V P. (2022) Analysis and design methods of helical piles: a critical review with emphasis on finite element method. J. Arabian Journal of Geosciences, 15(18): 1496.
5. DILEY L, HULSE L. (2007) Foundation design of wind turbines in Southwestern Alaska, a case study. In: Proceedings of the Arctic energy summit. Anchorage. Alaska. pp. 15-18.
6. Dong T W, Liang L, Wang W, et al. (2008) Experimental study on the interaction between blade and foundation of uplift spiral piles. J. Engineering Mechanics, 25(8): 150-155.
7. Dong T W, Zhang Y J, Liang L. (2011) Failure mechanism and bearing capacity design method of spiral pile foundation. Northeast University Press, Shenyang.
8. Dong T W, Liang L, Wang M S, etc. (2006) Screw pitch design and bearing capacity calculation of spiral pile under ultimate load. J. Geotechnical Engineering, 11: 2031-2034.

9. HAWKINS K, THORSTEN R. (2009) Load test results: large diameter helical pipe piles. In: Proceedings of the 2009 international foundation congress and equipment expo. New York: American Society of Civil Engineers. pp. 488-495.
10. Liu B K. (2019) Experimental study on blade-type steel pipe spiral pile and optimization of pile type parameters. J. Construction Techniques, 48(4): 93-97.
11. Li X Y, Yang Z P, Liu G, etc. (2023) Compression bearing capacity and frost-thaw resistance of isolated spiral pile. J. Geotechnical Engineering, 1-10.
12. Mahmood M R, Salim N M, Al-Gezzy A. (2021) Effect of soil saturation conditions and helical configurations on compression capacity of screw piles. J. IOP Conference Series.Materials Science and Engineering, 1058(1).
13. Malik A, Kuwano J, Tachibana S, et al. (2017) End bearing capacity comparison of screw pile with straight pipe pile under similar ground conditions. J. Acta Geotechnica, 12(2): 1-14.
14. Natnael T A, Lei G, Azizian M, et al. (2023) Field pull-out tests of percussion driven earth anchors (PDEAs). J. Applied Sciences, 13(4): 2132.
15. Peng L Y. (2020) Theory and technology of Vane type steel pipe spiral pile foundation. People's Communications Press, Beijing.
16. RAO, Narasimha S, PRASAD, et al. (1991) The Behaviour of Model Screw Piles IN Cohesive Soils. J. Geotechnical Society Thesis Papers.
17. SAKR M. (2009) Performance of helical piles in oil sand. J. Canadian Geotechnical Journal, 46(9): 1046-1061.
18. Stanier S A, Black J A, Hird C. (2014) Modelling helical screw piles in soft clay and design implications. J. Geotechnical Engineering, 167(5): 447-460.
19. Technical Code for Building Pile Foundation (JGJ94-2008). J. Construction Technology, 2012(Z 1): 38-39.
20. ZHANG D. (1999) Predicting capacity of helical screw piles in Alberta soils. D Edmonton: University of Alberta.